# An LPV Approach to Autonomous Vehicle Path Tracking in the Presence of Steering Actuation Nonlinearities

Matteo Corno, Giulio Panzani, Federico Roselli, Michele Giorelli, *Member, IEEE*, Davide Azzolini, and Sergio M. Savaresi

***Abstract*— This article deals with trajectory tracking for autonomous cars during evasive maneuvers and in the presence of steering actuator nonlinearities. This article develops an LPV MISO H-infinity controller based on the feedback of the lateral error at the center of gravity and the look-ahead distance. The controller architecture offers a way to cope with the effect of the steering nonlinearities, by scheduling one of the control weighting functions. A detailed experimental validation on three different maneuvers (straight driving, wide bend, and a double-lane change) shows the effectiveness of the proposed LPV solution.**

***Index Terms*— Autonomous automobiles, autonomous vehicles, power steering, vehicle dynamics.**

## I. Introduction

THE escalation toward higher levels of road vehicle autonomy is one of the main drivers of automotive research and is also heavily shaping the automotive industry. From the control point of view, most autonomous driving systems are categorized around two main subsystems: path planning and path tracking [1]. The former module, using environmental sensors and information, determines the desired path in global coordinates, which is an extremely rich and lively research field with many contributions (see [2]–[4]). The latter, the path tracking controller, acts on the vehicle actuators (steering, throttle, and braking) to track the reference path. This is usually achieved using inertial measurement and position information that can be obtained from fusing GPS, cameras, and other sensors. Two independent levels usually manage the path tracking task: a longitudinal controller (i.e., reference speed tracking) and lateral controller (i.e., reference path tracking).

Since the 1980s, when technology made it realistic, vehicle path tracking and, in particular, the lateral control problem has received thorough scientific scrutiny. The literature on this topic is vast. A great variety of control paradigms have been applied: among the most successful sliding mode control [5], nonlinear control [6], [7], potential field control [8]–[10], model predictive control [11]–[14], and optimal preview control [15], [16] can be listed. Besides the different approaches, the literature agrees on some points: the benefits introduced by a feedforward/preview term [17], the need of including the vehicle speed in the lateral control design, and that some level of look-ahead is essential (guaranteed by the access to the future planned path of the high-level controller) to provide accurate path tracking.

Regardless of the approach, the steer-by-wire actuator has a large impact on the path tracking controller: actuator dynamics, friction, and backlash limit the achievable performance. Not many publications explicitly account for this; notable exceptions are the experimental works by Gerdes' group [18], where the steer-by-wire system is modeled as a second-order system. However, the group employed a high performing steer-by-wire system that does not seem to use off-the-shelf components. The other relevant work in this direction is [19]: in this case, the steer nonlinearities are treated as a bounded disturbance, which is considered in the design of a linear controller.

This article focuses on path tracking in the case of evasive maneuvers and high-speed driving; in particular, we design a linear parameter varying (LPV) controller [20], [21] that achieves safe and efficient path tracking. The proposed strategy originates from the approach first introduced in [22], which reformulates the problem as the control of two variables: the lateral error at the vehicle center of gravity (CoG) and the derivative of the look-ahead error. Such an approach combines a rather simple controller structure with interesting tracking performance. In short summary, its relevance is the use of future information (provided by a look-ahead contribution) in a genuine feedback fashion (opposite to feedforward approaches that usually suffer the robustness issue), without the need of running online optimizations (that would be required by, e.g., an MPC approach); moreover, the resulting multiple-input single-output (MISO) controller is systematically designed by means of an H-infinity approach.

Unfortunately, the proposed controller does not address two important issues. The first one is that the variation of the vehicle speed is not taken into account in the controller design. The second is related to the performance of the low-level steering controller that highly influences the closed-loop performance and driving comfort; this second aspect is usually underestimated by the scientific literature but is expected to become increasingly important, given the maturity of the autonomous driving field.

Manuscript received August 16, 2019; revised May 1, 2020; accepted June 22, 2020. Date of publication July 13, 2020; date of current version June 10, 2021. Manuscript received in final form June 28, 2020. Recommended by Associate Editor A. Vahidi. *(Corresponding author: Matteo Corno.)*

Matteo Corno, Giulio Panzani, Federico Roselli, and Sergio M. Savaresi are with the Dipartimento di Elettronica, Informazione e Bioingegneria, Politecnico di Milano, 20133 Milan, Italy (e-mail: matteo.corno@polimi.it; giulio.panzani@polimi.it; federico.roselli@polimi.it; sergio.savaresi@polimi.it).

Michele Giorelli and Davide Azzolini are with Technology Innovation, Automated Driving Technologies, Magneti Marelli, 10078 Venaria Reale, Italy (e-mail: michele.giorelli@magnetimarelli.com; davide.azzolini@magnetimarelli.com).

Color versions of one or more of the figures in this article are available online at https://ieeexplore.ieee.org.

Digital Object Identifier 10.1109/TCST.2020.3006123

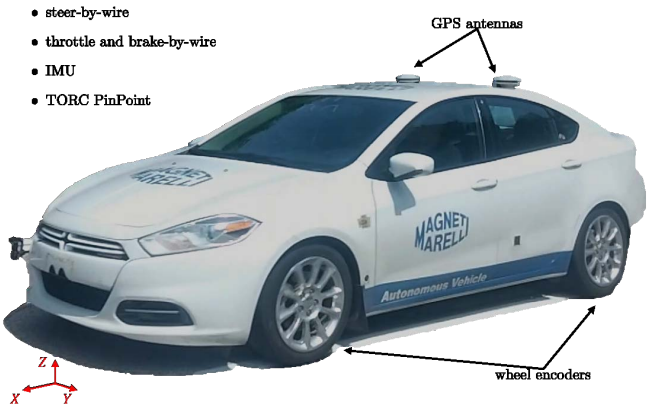


Fig. 1. Autonomous vehicle employed in this work.

TABLE I
VEHICLE PARAMETERS

| Parameter | Symbol | Value | Unit |
|---|---|---|---|
| Mass | $M$ | 1895 | Kg |
| Wheelbase | $L$ | 2.703 | m |
| Front axle-CoG distance | $l_f$ | 1.177 | m |
| Steering ratio | $n_{st0}$ | 1/14.54 | - |
| Wheel radius | $R_w$ | 0.31 | m |
| Yaw inertia | $J_z$ | 2400 | kgm$^2$ |
| Front cornering stiffness | $C_f$ | 124900 | N/rad |
| Rear cornering stiffness | $C_r$ | 166000 | N/rad |

In summary, this work extends the lateral controller [22] introducing gain scheduling. Such choice offers a way to systematically include two scheduling variables in the controller: the vehicle speed that naturally appears in the vehicle dynamics model, and the road curvature that helps to mitigate the effect of the steering actuator nonlinearities on the driving comfort. On the other side, the LPV extension does not alter the original controller structure preserving its discussed advantages. The controller extensions and design discussion are supported by simulation results and experiment tests on a test track with standard and dynamic maneuvers close to the handling limits.

## II. EXPERIMENTAL SETUP

All the results presented in this article refer to the vehicle shown in Fig. 1, i.e., a production Dodge Dart that has been retrofitted. Its main parameters are listed in Table I.

For the control of the longitudinal dynamics, the vehicle is equipped with a throttle-by-wire and a brake-by-wire system: the former, which is standard issue in the production vehicle, is controlled by overriding the command sent to the ECU; the latter is achieved by means of a linear actuator directly pushing the brake pedal. In order to enable the autonomous trajectory tracking, a steer-by-wire system is installed: it is composed of an electric motor connected to the standard steering column through a belt transmission. The steering angle is controlled by a third-party proprietary control system. The steering system, with its relevant nonlinearities, represents the limit of today's cost-effective technology, and addressing such limitation is an often underrated issue in the literature.

The vehicle is also equipped with the following sensors: an inertial measurement unit that provides the linear accelerations (longitudinal and lateral), four-wheel speed sensors, and a TORC Robotics PinPoint Localization and Precision IMU [23] that provides inertial measurements and, through sensor fusion, the position of the vehicle with an accuracy of 0.01 m at a rate of 100 Hz.

Regarding the autonomous driving control architecture, it is assumed that a high-level path planner provides the desired trajectory in global coordinates. Moreover, to ease the discussion, we further assume that the longitudinal speed control problem is solved and that the vehicle proceeds at the desired velocity.

## III. MODELING

This section recalls and validates the main control-oriented models employed in the remainder of this article. Following a bottom–up approach, we present the actuator, the vehicle dynamics, and the trajectory tracking model.

### A. Steer-by-Wire Model

It is a common practice, in the development of complex vehicle dynamics systems, to have several control layers: among the lowest, the actuator one is usually responsible for the sole control of the actuators. Its main objective is to guarantee a repeatable, with small steady-state error, and linear response of the actuator. A good actuator control needs to be robust to friction, backlashes, plays, and saturations that characterize the actuator. While the first two goals can be usually achieved by a proper application of standard linear control techniques, e.g., PD controllers [18], the last objective is more challenging, especially when changes of system parameters—due for example to aging and wearing—have to be accounted for. In this case, traditional control strategies yield repeatable, with small steady-state error, but mostly nonlinear responses; the nonlinearities are better addressed by more complex control structures, e.g., [24].

As denoted in Section II, a low-level proprietary controller is responsible for the position control of the steering column. In order to build a simulation-/control-oriented model, we use a gray-box approach. Fig. 2 shows the main elements that we consider in the model. It features a delay that accounts for the typical communication protocols between the central processing unit and the actuator driver, a position controller, modeled as a PID, and a second-order linear dynamic block that represents the mechanical dynamics of the steering column and, finally, a nonlinear Stribeck [25] friction block that accounts for the main nonlinearity.

Given the limited knowledge of the actuation system, all the model's parameters are identified through gray-box optimization. Two types of experiments are considered: a 10° amplitude sinusoidal oscillation, used to better characterize the stick-slip phenomena that arise because of the friction, and faster steps to assess the linear response when the friction is negligible compared with the inertial effects. Fig. 3 shows the comparison between the modeled steering wheel position and the measured one. The inspection of the experimental results validates the

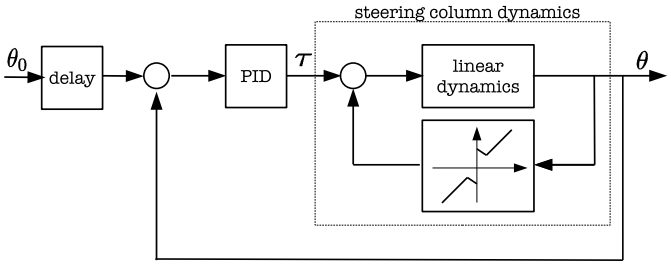


Fig. 2. Functional description of the steer-by-wire model.

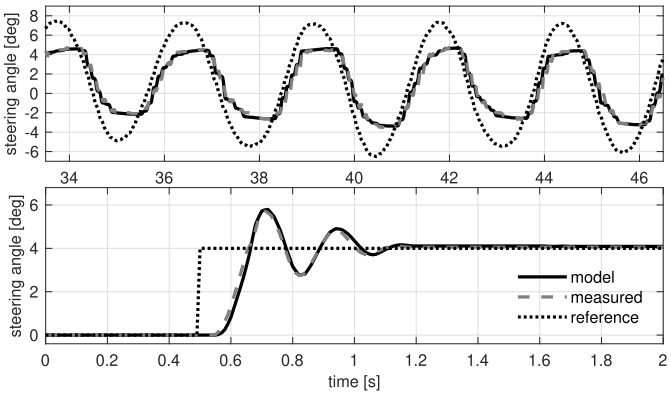


Fig. 3. Validation of the actuator model for slow (top) and fast (bottom) varying steering angles.

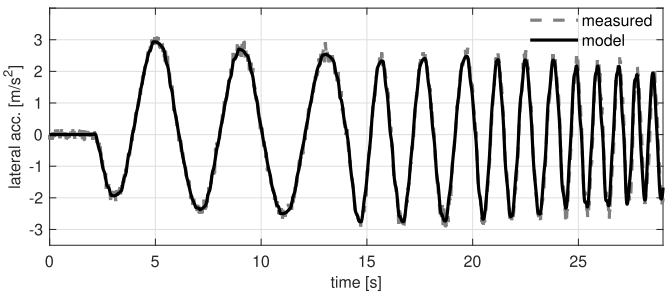


Fig. 4. Vehicle model validation with a steering sweep test at 70 km/h.

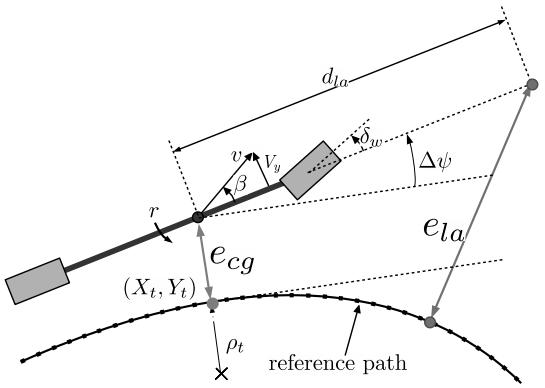


Fig. 5. Lateral error and look-ahead error definition.

effectiveness of the proposed steering system model, both for small and large excitations. Form the analysis, it is clear that the steering dynamics cannot be neglected: while, for slow actuation, the nonlinear static effects are more prominent, with evident stick-slip phenomena, for rapid actuation, the response is quite accurately described by a second-order delayed linear response.

### B. Vehicle Dynamics

The vehicle lateral dynamics are described by the classical single-track model [26] that assumes small steering angles, a path radius larger than the wheelbase, slowly varying speed, and linear tire characteristic. The model results in the following state-space equations:

$$\dot{V}_y = -\frac{C_f + C_r}{M\upsilon} V_y + \left(\frac{C_r l_r - C_f l_f}{M\upsilon} - \upsilon\right) r + \frac{C_f}{M}\delta_w$$
$$\dot{r} = \frac{C_r l_r - C_f l_f}{J_z}\beta - \frac{C_f l_f^2 + C_r l_r^2}{J_z \upsilon} r + \frac{C_f l_f}{J_z}\delta_w \qquad (1)$$

where $\upsilon$ is the velocity, $r$ is the yaw rate, $V_y$ is the lateral component of the velocity vector, $C_f$ and $C_r$ are, respectively, the front and rear cornering stiffness, $J_z$ is the total yaw inertia of the vehicle, $l_f$ and $l_r$ are the distances between the CoG and the front and rear axle, and $\delta_w$ is the steering angle at the wheels. Fig. 4 shows the plots of the validation of the model from the lateral acceleration point of view: the experiment is performed at 70 km/h with a sweep on the steering wheel, manually performed by the driver to exclude the nonlinear effects of the steer-by-wire system.

### C. Trajectory Tracking Model

The trajectory tracking model describes the evolution of the vehicle position with respect to the target path. The latter is well described by the reference path curvature $\rho_{\text{ref}}$, whereas the former is well characterized by means of the tracking error at the CoG, $e_{\text{cg}}$. Moreover, given its importance in the literature (see [27] and [28]), the look-ahead error $e_{\text{la}}$ is also introduced (as shown in Fig. 5). Assuming a small angular difference $(\Delta\psi)$ between the vehicle heading and the track yaw, the rate of change of the lateral error is computed as

$$\dot{e}_{\text{cg}} = \upsilon(\beta + \Delta\psi) \qquad (2)$$

with

$$\Delta\dot{\psi} = r - \rho_t \upsilon. \qquad (3)$$

Similarly, the state equation for the look-ahead error is

$$\dot{e}_{\text{la}} = \dot{e}_{\text{cg}} + d_{\text{la}}\Delta\dot{\psi} = \upsilon(\beta + \Delta\psi) + d_{\text{la}}(r - \rho_{\text{ref}}\upsilon). \qquad (4)$$

The vehicle and the path tracking dynamics (1)–(4) are summarized in the compact form (5), as shown at the bottom of the next page.

The overall system is multiple-input multiple-output, where the inputs are the controllable steering angle and the known reference curvature (computed at the nearest point on the reference path). The CoG error is one output of the system; in addition, the time derivative of the error at the look-ahead distance is included as a controller output.

The look-ahead distance $d_{\text{la}}$ and the vehicle speed $\upsilon$ can be considered parameters: the former is a tuning parameter, whereas the latter is a measurable time-varying one.

## IV. LPV Path Tracking Control

### A. Controller Description

As discussed in Section I, the present work extends [22], where a linear H-infinity path tracking controller is based on the feedback of two variables: the lateral tracking error and the derivative of the look-ahead one. In spite of its simplicity, the controller shows excellent tracking performance on real autonomous driving tests.

Unfortunately, it does not address two important issues. The first one is related to vehicle speed that, as shown in Section III, influences the tracking dynamics. This is a known issue, and it is widely accepted that in order to achieve an adequate level of performance, especially for dynamic maneuvers, the vehicle speed must be taken into account.

The second issue is related to the behavior of the low-level steering controller. Indeed, the original controller assumes that all the involved dynamics are linear, including the actuator ones. However, Section III shows that the linear model is valid only when the steering is actuated with sufficiently high speed, but when the steering rates are low, friction nonlinearities play an important role. It is, therefore, expected that during, for example, straight driving, the closed-loop performance will not match the design specifications. To better catch the relevance of the actuator nonlinearities on the vehicle tracking behavior, Fig. 6 shows the results of a closed-loop (using the discussed controller [22]) simulation during straight driving with and without the inclusion of the actuator frictions. In the linear case, as expected, the response settles to the null tracking error and the steering angle to zero. When friction is included, the system exhibits a limit cycle where the error and the steer continue to oscillate. As further validation, real data from an analogous experiment are added to the plot for comparison: notice that being a closed-loop test, the time-domain trajectories are different, but the amplitude and the frequency of the oscillations resemble and validate the simulated ones.

The LPV framework can address both issues. In fact, the controller is an output feedback controller whose parameters are automatically "gain-scheduled" according to the time-varying values assumed by a set of parameters $p(t)$. In the LPV framework, it is described by the following equations:

$$\begin{cases} \dot{\zeta} = A_k(p)\zeta + B_k(p)y \\ u = C_k(p)\zeta + D_k(p)y \end{cases} \tag{6}$$

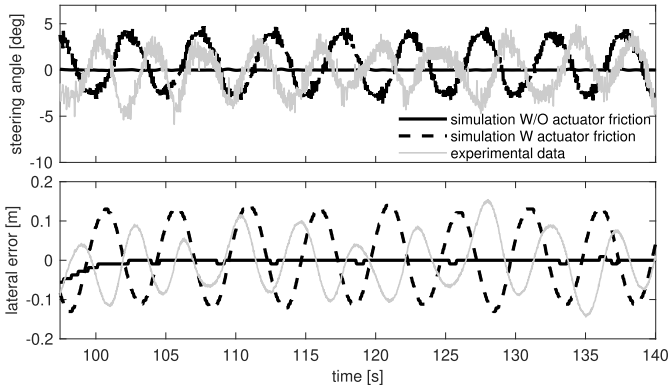


Fig. 6. Effect of the actuator nonlinearities on the driving performances.

where the system matrices linearly depend on the polytopic coordinates (marked with $\Pi_i$)

$$\begin{bmatrix} A_k(p) & B_k(p) \\ C_k(p) & D_k(p) \end{bmatrix} = \sum_{i=1}^{q} \alpha_i(p) \begin{bmatrix} A_k(\Pi_i) & B_k(\Pi_i) \\ C_k(\Pi_i) & D_k(\Pi_i) \end{bmatrix}. \tag{7}$$

The LPV controller can be designed to ensure closed-loop stability and to minimize a quadratic $\mathcal{H}_\infty$ performance by solving a system of linear matrix inequalities (see [29] for further details). This can be done if the controlled system dynamics can be expressed as an LPV plant and providing possibly parameter dependent (see [30]) dynamic weights that define the desired performances.

The block diagram of overall control scheme, meant for the H-infinity control design, is represented in Fig. 7. It features (from left to right) the controller $K(s, p)$, the linear steering-actuator dynamics augmented with Padé approximation of the delay $G_{SW}(s)$, the vehicle and trajectory tracking model $G_V(s, p)$, and the effect of the reference path curvature $G_\rho(s, p)$ on CoG error.

Five dynamic weights are introduced to shape the closed-loop properties of the controlled system.

1) $W_{e_{\rm cg}}(s)$ shapes the closed-loop sensitivity referred to the lateral error $e_{\rm cg}$.
2) $W_{\dot{e}_{\rm la}}(s)$ shapes the closed-loop sensitivity referred to the look-ahead error derivative $\dot{e}_{\rm la}$.
3) $W_{act}(s)$ shapes the control effort sensitivity. Its main objective is to avoid high-frequency actuation that the steer-by-wire would not be able to track.

$$\begin{bmatrix} \dot{V}_y \\ \dot{r} \\ \Delta\dot{\psi} \\ \dot{e}_{\rm cg} \end{bmatrix} = \begin{bmatrix} -\dfrac{C_f + C_r}{Mv} & \dfrac{C_r l_r - C_f l_f}{Mv} - v & 0 & 0 \\ \dfrac{C_r l_r - C_f l_f}{J_z v} & -\dfrac{C_f l_f^2 + C_r l_r^2}{J_z v} & 0 & 0 \\ 0 & 1 & 0 & 0 \\ 1 & 0 & v & 0 \end{bmatrix} \begin{bmatrix} V_y \\ r \\ \Delta\psi \\ e_{\rm cg} \end{bmatrix} + \begin{bmatrix} \dfrac{C_f}{M} & 0 \\ \dfrac{C_f l_f}{J_z} & 0 \\ 0 & -v \\ 0 & 0 \end{bmatrix} \begin{bmatrix} \delta_w \\ \rho_{\rm ref} \end{bmatrix}$$

$$\begin{bmatrix} y_1 \\ y_2 \end{bmatrix} = \begin{bmatrix} 0 & 0 & 0 & 1 \\ 1 & d_{\rm la} & v & 0 \end{bmatrix} \begin{bmatrix} V_y \\ r \\ \Delta\psi \\ e_{\rm cg} \end{bmatrix} + \begin{bmatrix} 0 & 0 \\ 0 & -d_{\rm la} v \end{bmatrix} \begin{bmatrix} \delta_w \\ \rho_{\rm ref} \end{bmatrix} \tag{5}$$

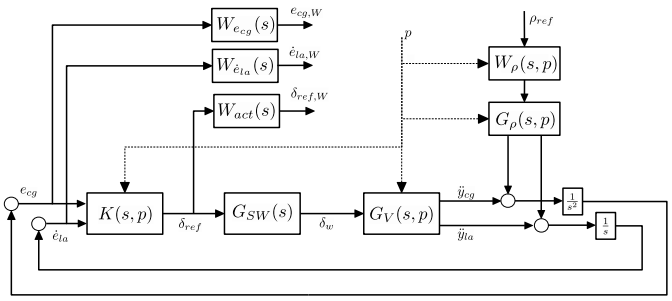


Fig. 7. LPV closed-loop control scheme of the combined CoG and look-ahead strategy.

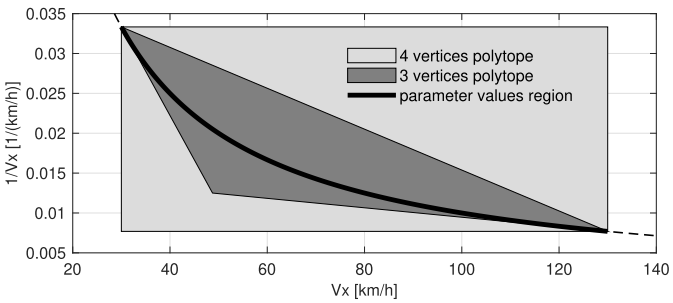


Fig. 8. Polytopes for the velocity parameter space description. The black line is the curve of the possible values assumed by the (not independent) parameters.

4) $W_\rho(s, p)$ weighs the effect of the disturbance in the loop; it is chosen as a first-order filter replicating the maximum frequency content of an aggressive maneuver.

Compared with the control scheme previously proposed in [22], consistently with the LPV framework, some components of the block diagram are now dependent on the parameters vector $p$ (time dependence has been omitted for simplicity): the self-scheduled controller $K(s, p)$ but also the system dynamics $G_V(s, p)$ and $G_\rho(s, p)$ and the weighting function $W_\rho(s, p)$. The selected time-varying parameters $p$ are related to the vehicle speed and the target path curvature: they are precisely introduced in the following.

*1) Velocity Scheduling:* The influence of the vehicle speed is recast in the LPV framework by inspecting the system equations (5). Despite that the system matrices are not linearly dependent on the longitudinal speed a convenient, albeit conservative, affine description of the system is possible considering $v$ and $1/v$ as two independent parameters. Within this perspective, the vehicle and trajectory tracking dynamics can be written as a combination of three matrices

$$\dot{x} = \left(A_0 + A_1\frac{1}{v} + A_2 v\right)x + \left(B_0 + B_1\frac{1}{v} + B_2 v\right)u$$
$$y = \left(C_0 + C_1\frac{1}{v} + C_2 v\right)x + \left(D_0 + D_1\frac{1}{v} + D_2 v\right)u \quad (8)$$

where

$$A_0 = \begin{bmatrix} 0 & 0 & 0 & 0 \\ 0 & 0 & 0 & 0 \\ 0 & 1 & 0 & 0 \\ 1 & 0 & 0 & 0 \end{bmatrix}, \quad A_2 = \begin{bmatrix} 0 & -1 & 0 & 0 \\ 0 & 0 & 0 & 0 \\ 0 & 0 & 0 & 0 \\ 0 & 0 & 1 & 0 \end{bmatrix}$$
$$A_1 = \begin{bmatrix} -\dfrac{C_r + C_f}{M} & \dfrac{C_r l_r - C_f l_f}{M} & 0 & 0 \\ \dfrac{C_r l_r - C_f l_f}{J_z} & -\dfrac{C_r l_r^2 + C_f l_f^2}{J_z} & 0 & 0 \\ 0 & 0 & 0 & 0 \\ 0 & 0 & 0 & 0 \end{bmatrix}$$
$$B_0 = \begin{bmatrix} \dfrac{C_f}{M} & 0 \\ \dfrac{C_f l_f}{J_z} & 0 \\ 0 & 0 \\ 0 & 0 \end{bmatrix}, \quad B_1 = \underline{0} \quad B_2 = \begin{bmatrix} 0 & 0 \\ 0 & 0 \\ 0 & 1 \\ 0 & 0 \end{bmatrix}$$

$$C_0 = \begin{bmatrix} 0 & 0 & 0 & 1 \\ 1 & d_{\text{la}} & 0 & 0 \end{bmatrix}, \quad C_1 = \underline{0} \quad C_2 = \begin{bmatrix} 0 & 0 & 0 & 0 \\ 0 & 0 & 1 & 0 \end{bmatrix}$$
$$D_0 = \underline{0} \quad D_1 = \underline{0} \quad D_2 = \begin{bmatrix} 0 & 0 \\ 0 & -d_{\text{la}} \end{bmatrix}. \quad (9)$$

This description of the controller dynamics allows one to easily include the velocity effect in the LPV controller, by means of the LMI design [29]. In addition, to reduce the conservativeness coming from the use of two nonindependent parameters, their dependence is, in fact, exploited describing the parameter space with a three-vertex polytope (opposite to the four-vertex polytope standardly used for truly independent parameters), see Fig. 8. It is interesting to note that, in view of the classical two-independent-controller architecture (lateral and longitudinal), the path tracking controller will be exposed to relatively slow variations of velocity during aggressive maneuvers. In fact, it is common practice to decouple the braking (or acceleration) and steering phases of evasive maneuvers.

*2) Curvature Scheduling:* A cost-effective control-based solution is here proposed to cope with the undesired effects induced by the servo-controller nonlinearities shown in Fig. 6, still preserving the linear controller structure. Such a solution is based on the evidence that the properties of the limit cycle induced by the steer-by-wire actuator are significantly affected by the trajectory tracking control bandwidth. Its effects are summarized by the experimental results presented in Fig. 9 (also supported by simulations, here omitted for the sake of conciseness), where the spectra of the lateral acceleration and the tracking error at the CoG are shown for a straight run experiment at 85 km/h, with different control bandwidths. The controller bandwidth has an impact on the tracking error but, more interestingly, on the perceived driving comfort here represented with the lateral acceleration. In particular, for a high bandwidth controller, not only the acceleration values increase but mainly focus around 0.5 Hz, a frequency at which passengers are particularly sensitive. Opposite to the lowest bandwidth yields a slightly larger tracking error (still below 15 cm) but a considerable reduction in both the amplitude and frequency of the lateral acceleration. This analysis proves that a different controller tuning can improve comfort with a limited effect on tracking performance during straight driving.

Unfortunately, detuning the controller during transient and cornering maneuvers leads to unacceptable tracking errors.

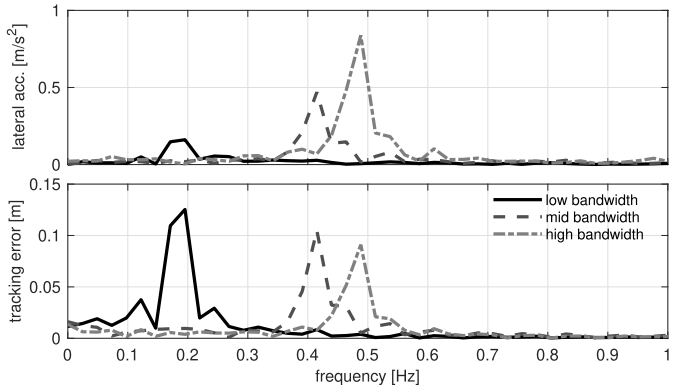


Fig. 9. Spectra of the lateral acceleration and tracking error obtained during a 20-s experiment at 85 km/h.

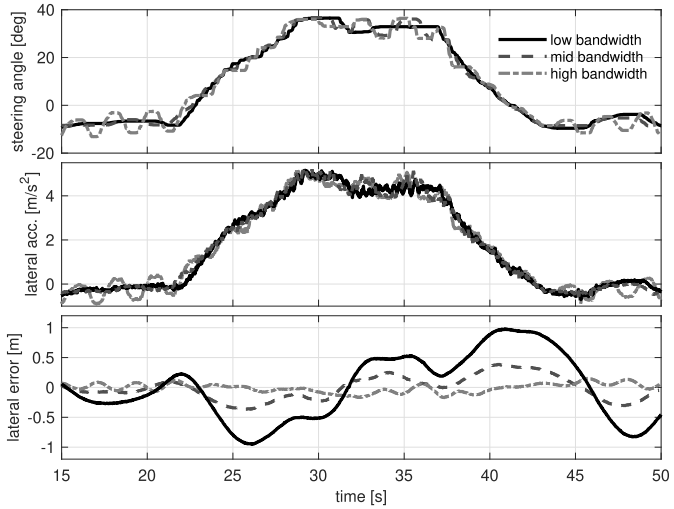


Fig. 10. Steering angle and tracking error for a wide bend at 70 km/h.

This is shown in Fig. 10, where a wide bend with a constant radius of 70 m is performed varying the controller bandwidth: the tracking error reaches values of around 1 m for the lowest tuning.

Unexpectedly, a tradeoff arises: the lateral errors reached for the detuned case are compatible with rectilinear driving requirements but do not guarantee a safe execution of transient and cornering maneuvers. To systematically solve this tradeoff, the proposed solution is to modify the controller bandwidth depending on whether the vehicle is negotiating a corner or not. Additional scheduling implements this idea: the weighting function $W_\rho(s, p)$ is adapted according to the variation of a parameter $\alpha$, which indicates whether the vehicle is cornering or not; in particular, $W_\rho(s, p)$ is designed so that its pole frequency is reduced when straight driving is ongoing. Acting on the weighting functions $W_\rho(s, p)$ rather than on the more intuitive $W_{e_{\rm cg}}(s)$ and $W_{\dot{e}_{\rm la}}(s)$ helps to reduce the tuning efforts, still yielding the desired bandwidth modification. In fact, lowering the bandwidth of $W_\rho(s, p)$ implies that the effect of a disturbance (the curvature, as shown in Fig. 7) is considered less important at higher frequency, leading to a less reactive (i.e., with lower bandwidth) controller.

TABLE II
CONTROLLER PARAMETERS

| | |
|---|---|
| $W_{e_{cg}} = \frac{0.01s+0.632}{s+0.0632}$ | $W_{\dot{e}_{la}} = \frac{0.99s+0.267}{s+0.0267}$ |
| $W_{act} = \frac{s+130}{s+1441}$ | $d_{la} = 12$ [m] |
| $W_\rho = 0.02\frac{1+s/(2\pi 100 f_\rho)}{1+s/(2\pi f_\rho)}$ | $f_\rho = 0.0475\alpha + 0.0025$ [Hz] |

A good candidate for the parameter $\alpha$ could be the reference curvature. However, if only the current curvature were considered, the controller would be affected by a delay, i.e., the vehicle would start negotiating aggressive maneuvers with a tuning close designed for straight driving. Thus, the actual scheduling parameter $\alpha$ is computed linearly remapping the path curvature $\rho_{\rm ref}$ into the variable $\tilde{\rho}_{\rm ref} \in [0, 1]$ so that $\rho_{\rm ref,min} = 0$, $\rho_{\rm ref,max} = 1$, and saturating the result

$$\alpha(t) = \text{sat}_{[0,1]}(\tilde{\rho}_{\rm ref}). \tag{10}$$

The values of $\alpha$ must be interpreted so that 0 refers to straight driving and 1 to turning. In order to reduce the effect of noise and outliers in the target path definition, the reference curvature is averaged in the time window $t \in [-T_{\rm past}, T_{\rm preview}]$ before computing $\tilde{\rho}_{\rm ref}$, taking advantage of the future values of the reference trajectory.

The reference path curvature scheduling is the central idea that makes the proposed approach different from [19], which is, to the best of our knowledge, the only work that explicitly considers a nonideal steer-by-wire in the control design. Besides minor differences in the context (e.g., the mentioned work does not explicitly address the autonomous path tracking problem but refers to a generic longitudinal speed–yaw rate control problem), the most important one is how authors treat the steer backlash hysteresis, as a bounded disturbance linearly entering the plant and including its effect in a performance norm minimization problem. In our approach, in fact, we opt for varying importance of the effect of the steer nonlinearities, depending on the type of reference trajectory, and we modify the controller tuning accordingly.

In conclusion, referring to the overall control architecture of Fig. 7, the parameter vector $p(t)$ is

$$p = \left[\frac{1}{v}, \quad v, \quad \alpha\right]$$

and the number of vertices $q$ in (7) results equal to 6.

## V. EXPERIMENTAL VALIDATION

### A. Controller Tuning

In the following, we validate the controller in different scenarios on the instrumented vehicle. Table II lists the values of controller parameters.

The parameter tuning has been performed sequentially.

1) Tuning of the weighting functions, with the look-ahead distance of 9 m (consistent with from previous scientific literature, e.g., [17]).
2) Tuning of the look-ahead distance.

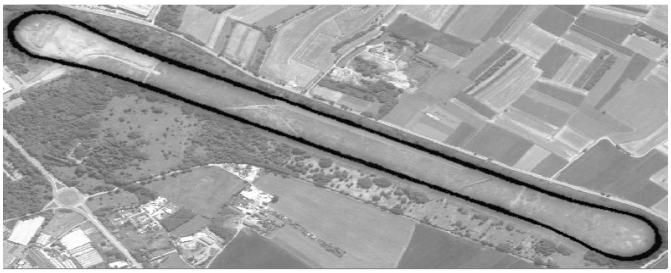

Fig. 11. Autonomous driving test track.

3) Design and curvature scheduling of $W_\rho(s,\alpha)$; notice that the speed scheduling is naturally "embedded" in the LPV structure of the controlled plant and does not require any further tuning.

Even if the sequential tuning does not offer any guarantee of optimality, simulations and experimental tuning always led to tracking performance increase at each step, yielding to overall satisfactory results.

Regarding the weighting functions, a pole/zero structure has been found sufficient to achieve satisfactory results. $W_{\dot{e}_{\rm la}}(s)$ dominates at higher frequencies compared with $W_{e_{\rm cg}}(s)$, given its "prediction" role within the control law. Consistently with the low-level position in the control law hierarchy, the actuator weighting function has the highest bandwidth.

The look-ahead tuning optimizes the following tradeoff: for short look-ahead distances, the vehicle reacts too late when changes in the target trajectory occur; too long distances cause the vehicle to anticipate the maneuver and "cutting corners." The proposed value averages the experimental results on different maneuvers.

Finally, the curvature scheduling is obtained by changing the pole/zero frequency of $W_\rho(s,\alpha)$, namely, $f_\rho$ (see Table II) according to the curvature [through the parameter $\alpha$, see (10)]. First, fixed values of $f_\rho$ are found to yield the desired performance during straight driving and cornering: for the former, a value of $f_\rho = 0.0025$ Hz is found (corresponding to the "low bandwidth" case of Fig. 9), and for the latter, a value of $f_\rho = 0.05$ Hz (the "high bandwidth" case of Fig. 10). The scheduling is then obtained with a linear transition between these two values, as function of the parameter $\alpha$.

### B. Results

The proposed controller is tested against two different scenarios. The first one is the track shown in Fig. 11 that features two wide bends and connecting straights, mainly meant to verify the effect of the curvature scheduling and the overall performances. Fig. 12 shows one full lap at 80 km/h proving how the curvature-based scheduling improves the oscillations on the straight sections without deteriorating the cornering capabilities. Fig. 12 shows two sets of data: a test in which only the velocity scheduling is active and a second test in which the full scheduling is used. As expected, based on the discussion of Section IV, one can see that the full scheduling yields an accurate tracking of the trajectory during cornering and comfortable straight driving with limited lateral

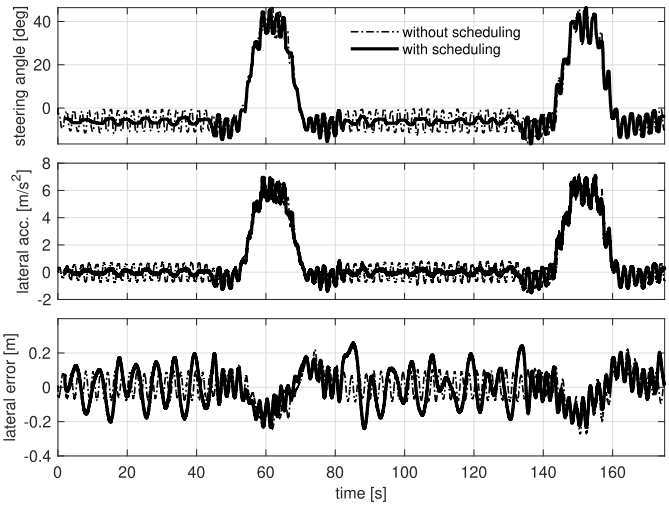


Fig. 12. Comparison between the fully (velocity and curvature) scheduled controller and the velocity only scheduled controller.

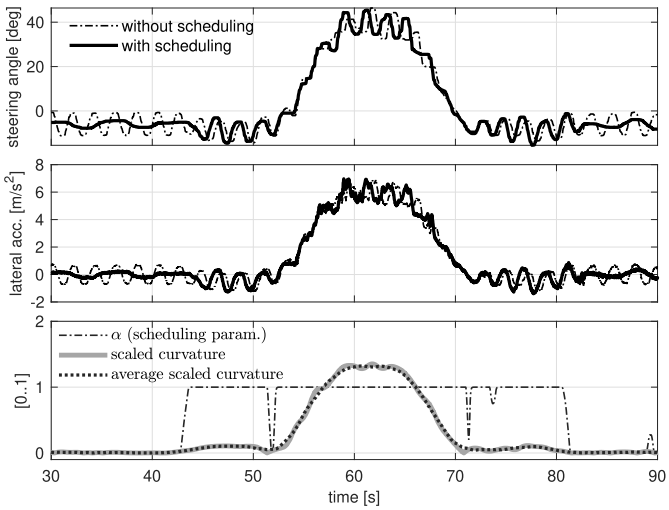


Fig. 13. Details on the transition phase from straight to cornering.

acceleration. The transition phase from straight driving to cornering is detailed in Fig. 13: in particular, the bottom plot shows the scheduling variable $\alpha$, the scaled path curvature, and the average one. The use of future—available—target trajectory values effectively includes an equivalent acausal filtered curvature signal where noise has been cleaned out without introducing time delays. Notice that in this experiment, the transition phase is relatively rapid and well managed by the scheduling: the employed LPV approach ensures the stability of the closed-loop system.

The second maneuver is the double-lane change (DLC) performed at a different speed (ranging from 50 to 90 km/h), meant to validate the controller performances for highly dynamic maneuvers. Fig. 14 compares the simulated and the experimental results in terms of tracking root-mean-squared error at different speeds (maximum lateral accelerations are also provided in the right plots for a better experiment contextualization), which, when the LPV controller is used, keeps almost constant and limited to satisfactory values. To better

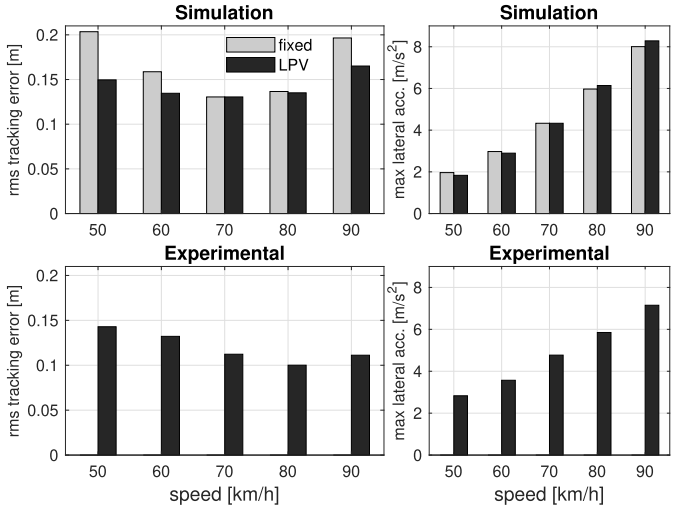


Fig. 14. Tracking rms error (left) and maximum lateral acceleration (right) for the simulated (top) and experimental (bottom) DLC maneuver.

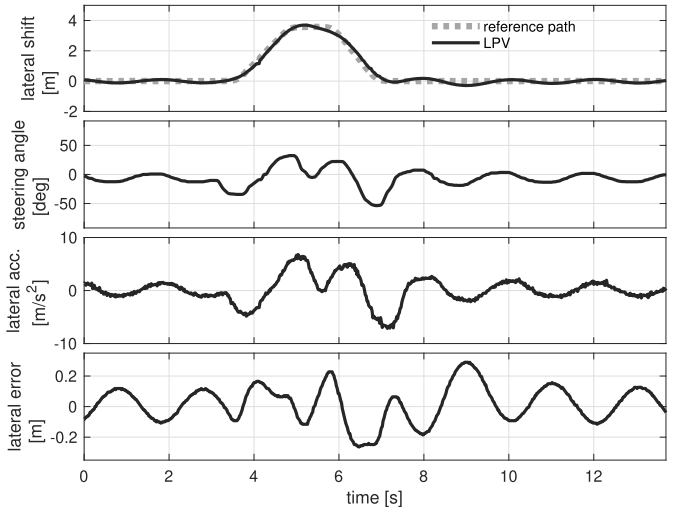


Fig. 15. LPV controller behavior on the DLC maneuver at 90 km/h.

appreciate the effect of the speed scheduling, the DLC maneuver is also simulated for a fixed controller tuning (at a nominal speed of 70 km/h), yielding to higher and more variable rms values. To show the good performance achieved with the proposed controller, the time-domain plots for the DLC at 90 km/h are provided in Fig. 15. In this test, the maximum tracking error is always less than 0.3 m (and, in general, never higher than 0.6 m also for different speed values). As a side comment, it is worthy to highlight that the controller—designed using a linear vehicle model—proves robust enough to achieve good tracking performances also in the proposed scenario, where a lateral acceleration of 0.8 g and a sideslip angle of 2.5° indicate proximity to the tire saturation condition.

## VI. Conclusion

This article discusses the design, implementation, and validation of a trajectory tracking system for autonomous cars. The main focus is on guaranteeing adequate tracking performance also in the case of aggressive maneuvers, considering steering actuator nonlinearities, relevant also for nonprototypal vehicles, and possibly varying vehicle speed. This objective is reached without introducing optimization-based controllers

The solution consists of the LPV extension of a MIMO-LPV controller, proposed in [22], that makes it possible to consider the objective of controlling both the lateral error at the CoG and its derivative at the look-ahead distance. This yields the ability to perform aggressive maneuvers as well as steady state, cornering with small tracking errors.

The LPV nature is useful to systematically account for the vehicle dynamics dependence on the longitudinal velocity and also the nonlinearities in the steering actuators. This article provides a detailed discussion of the steering actuator model and the limit cycle that stems from the friction and backlash in the actuator. From a pure control system design point of view, the issue can be addressed by scheduling the bandwidth of the controller according to the curvature. The scheduling shifts the limit cycle to amplitudes and frequencies that are not uncomfortable for the passengers when accurate tracking is not necessary.

Detailed experimental validation on an instrumented vehicle, against three different types of maneuvers (straight driving, bends, and DLC), proves that the controller can successfully negotiate the maneuvers with a tracking error of less than 40 cm even in cases with a lateral acceleration of 0.8 g. This performance is deemed adequate for an autonomous driving scenario. Controller parameters and general guidelines on their tuning are given to encourage scientific comparison and practical employment.

In conclusion, this article shows that adequate tracking performance can be achieved in a realistic and challenging setting without using optimization-based controllers with their burden of complexity and computational demands

Future work will focus on the generation of a feasible trajectory for efficient, safe, and stable obstacle avoidance.

## References

[1] D. Gonzalez, J. Perez, V. Milanes, and F. Nashashibi, "A review of motion planning techniques for automated vehicles," *IEEE Trans. Intell. Transp. Syst.*, vol. 17, no. 4, pp. 1135–1145, Apr. 2016.

[2] A. Broggi *et al.*, "Extensive tests of autonomous driving technologies," *IEEE Trans. Intell. Transp. Syst.*, vol. 14, no. 3, pp. 1403–1415, Sep. 2013.

[3] C. Katrakazas, M. Quddus, W.-H. Chen, and L. Deka, "Real-time motion planning methods for autonomous on-road driving: State-of-the-art and future research directions," *Transp. Res. C, Emerg. Technol.*, vol. 60, pp. 416–442, Nov. 2015.

[4] D. Ferguson, T. M. Howard, and M. Likhachev, "Motion planning in urban environments," *J. Field Robot.*, vol. 25, nos. 11–12, pp. 939–960, Nov. 2008.

[5] J. Guldner, V. I. Utkin, and J. Ackermann, "A sliding mode control approach to automatic car steering," in *Proc. Amer. Control Conf. (ACC)*, vol. 2, 1994, pp. 1969–1973.

[6] M. Schorn, U. Stahlin, A. Khanafer, and R. Isermann, "Nonlinear trajectory following control for automatic steering of a collision avoiding vehicle," in *Proc. Amer. Control Conf.*, 2006, p. 6.

[7] S. C. Peters, E. Frazzoli, and K. Iagnemma, "Differential flatness of a front-steered vehicle with tire force control," in *Proc. IEEE/RSJ Int. Conf. Intell. Robots Syst.*, Sep. 2011, pp. 298–304.

[8] J. C. Gerdes and E. J. Rossetter, "A unified approach to driver assistance systems based on artificial potential fields," *J. Dyn. Syst., Meas., Control*, vol. 123, no. 3, pp. 431–438, Sep. 2001.

[9] E. J. Rossetter, J. P. Switkes, and J. C. Gerdes, "Experimental validation of the potential field lanekeeping system," *Int. J. Automot. Technol.*, vol. 5, no. 2, pp. 95–108, 2004.

[10] K. Kritayakirana, "Autonomous vehicle control at the limits of handling," Ph.D. dissertation, Dyn. Des. Lab., Stanford Univ., Stanford, CA, USA, 2012.
[11] C. E. Beal and J. C. Gerdes, "Model predictive control for vehicle stabilization at the limits of handling," *IEEE Trans. Control Syst. Technol.*, vol. 21, no. 4, pp. 1258–1269, Jul. 2013.
[12] P. Falcone, F. Borrelli, J. Asgari, H. E. Tseng, and D. Hrovat, "Predictive active steering control for autonomous vehicle systems," *IEEE Trans. Control Syst. Technol.*, vol. 15, no. 3, pp. 566–580, May 2007.
[13] F. Borrelli, P. Falcone, T. Keviczky, J. Asgari, and D. Hrovat, "MPC-based approach to active steering for autonomous vehicle systems," *Int. J. Veh. Auto. Syst.*, vol. 3, nos. 2–4, pp. 265–291, 2005.
[14] J. Liu, P. Jayakumar, J. L. Stein, and T. Ersal, "Combined speed and steering control in high-speed autonomous ground vehicles for obstacle avoidance using model predictive control," *IEEE Trans. Veh. Technol.*, vol. 66, no. 10, pp. 8746–8763, Oct. 2017.
[15] P. Symonds, R. S. Sharp, and D. Casanova, "A mathematical model for driver steering control, with design, tuning and performance results," *Vehicle Syst. Dyn.*, vol. 33, no. 5, pp. 289–326, May 2000.
[16] M. Thommyppillai, S. Evangelou, and R. S. Sharp, "Car driving at the limit by adaptive linear optimal preview control," *Vehicle Syst. Dyn.*, vol. 47, no. 12, pp. 1535–1550, Dec. 2009.
[17] N. R. Kapania and J. C. Gerdes, "Design of a feedback-feedforward steering controller for accurate path tracking and stability at the limits of handling," *Vehicle Syst. Dyn.*, vol. 53, no. 12, pp. 1687–1704, Dec. 2015.
[18] P. Yih and J. C. Gerdes, "Modification of vehicle handling characteristics via steer-by-wire," *IEEE Trans. Control Syst. Technol.*, vol. 13, no. 6, pp. 965–976, Nov. 2005.
[19] X. Huang, H. Zhang, G. Zhang, and J. Wang, "Robust weighted gain-scheduling H∞ vehicle lateral motion control with considerations of steering system backlash-type hysteresis," *IEEE Trans. Control Syst. Technol.*, vol. 22, no. 5, pp. 1740–1753, Sep. 2014.
[20] F. Wu, "Control of linear parameter varying systems," Ph.D. dissertation, Dept. Mech. Eng., Univ. California, Berkeley, CA, USA, 1995.
[21] P. Gahinet, P. Apkarian, and M. Chilali, "Affine parameter-dependent Lyapunov functions and real parametric uncertainty," *IEEE Trans. Autom. Control*, vol. 41, no. 3, pp. 436–442, Mar. 1996.
[22] F. Roselli *et al.*, "$H_\infty$ control with look-ahead for lane keeping in autonomous vehicles," in *Proc. IEEE Conf. Control Technol. Appl. (CCTA)*, Aug. 2017, pp. 2220–2225.
[23] *Torc Robotics*. Accessed: Jul. 7, 2020. [Online]. Available: https://torc.ai/
[24] Z. Sun, J. Zheng, Z. Man, and H. Wang, "Robust control of a vehicle steer-by-wire system using adaptive sliding mode," *IEEE Trans. Ind. Electron.*, vol. 63, no. 4, pp. 2251–2262, Apr. 2016.
[25] G. Panzani, M. Corno, and S. M. Savaresi, "On adaptive electronic throttle control for sport motorcycles," *Control Eng. Pract.*, vol. 21, no. 1, pp. 42–53, Jan. 2013.
[26] R. Rajamani, *Vehicle Dynamics and Control*. Springer, 2011.
[27] J. Guldner, H.-S. Tan, and S. Patwardhan, "On fundamental issues of vehicle steering control for highway automation," California PATH Program, Inst. Transp. Stud., Univ. California, Berkeley, CA, USA, Tech. Rep. UCB-ITS-PWP-97-11, 1997.
[28] P. Hingwe and M. Tomizuka, "A variable look-ahead controller for lateral guidance of four wheeled vehicles," in *Proc. Amer. Control Conf. (ACC)*, vol. 1, Jun. 1998, pp. 31–35.
[29] P. Apkarian, J.-M. Biannic, and P. Gahinet, "Self-scheduled H-infinity control of missile via linear matrix inequalities," *J. Guid., Control, Dyn.*, vol. 18, no. 3, pp. 532–538, May 1995.
[30] F. Wu, K. M. Grigoriadis, and A. Packard, "Anti-windup controller design using linear parameter-varying control methods," *Int. J. Control*, vol. 73, no. 12, pp. 1104–1114, Jan. 2000.